Resonant tunneling in a quantum step: Inverse photoemission spectroscopy of Ag/Al(100)

J. F. Veyan[1,2] and P. Häberle[1,*]
[1]*Departamento de Física, Universidad Técnica Federico Santa María, Casilla 110-V, Valparaíso, Chile*
[2]*Instituto de Física, Universidad Católica de Valparaíso, Av. Brasil 1018, Valparaíso, Chile*
(Received 24 May 2005; published 2 August 2005)

Inverse photoemission spectroscopy has been used to study the electronic structure of thin Ag layers adsorbed on Al(100). The experimental thickness dependence of the emitted photon intensities is described in terms of quantum size effects in a one-dimensional system. The quantum confinement displayed by our data originates in the reflection from a barrier-less electronic potential, at the Ag/Al interface. One of the electronic features displays a resonant tunneling behavior associated with transmission through an energy gap of the metallic thin film.

DOI: 10.1103/PhysRevB.72.073401 PACS number(s): 73.20.At, 73.21.Fg, 79.60.−i

Among the systems in which quantum size effects (QSE) have been studied, those formed by thin atomic Ag layers[1] have attracted great interest in recent years.[2–4] Characterization techniques such as photoemission[3] and scanning probe microscopy[4] have been used to examine both their electronic and geometrical structure. The main quantization effect explored, in these and other similar overlayers, has been the formation of quantum well resonances (QWr). They have been shown to influence many nanoscale properties such as giant magneto resistance, structural stability of thin films, thickness dependence in electronic transport, and chemisorption, among others. These QW-induced changes in the local density of states (DOS) have been mostly detected as resonances in photoemission experiments, and a few of them by inverse photoemission spectroscopy (IPS). The valence-band electrons display, in addition to the atomic quantization, a confinement induced by the thin layer. The confining potential well is formed between the vacuum barrier in one side and by the strong scattering at the interface [Fig. 1(a)], due to an abrupt change in the potential energy. The origin of the repulsion at the interface has been attributed to effects such as the existence of an energy gap in the substrate bulk energy bands, and/or a mismatch in the lattice parameters between overlayer and substrate.[1,5] Many of the systems displaying these resonances are the so-called metallic quantum wells (mQWs). They are formed by metallic overlayers with a high density of well-delocalized *s-p* electrons in the valence band.[1,5–10]

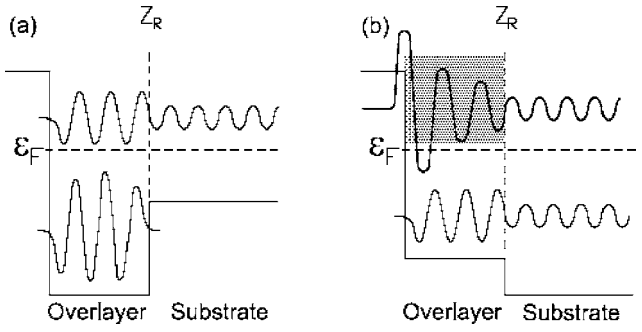

FIG. 1. Different types of potentials giving rise to QSE. The gray areas represent energy band gaps. Z_R is the reflection point for the electronic wave function. The diagram also shows general features of a few wave function solutions for different energies. (a) corresponds to the standard model for mQWs potentials; (b) model for a barrier-less type potential, with a band gap in the overlayer, as in Ag/Al(100).

In this study we present a different type of quantization effect. The potential energy at the interface can be described in terms of a potential step [Fig. 1(b)]. These types of quantization, which are not as strong as regular mQW, have been reported previously in overlayer–substrate systems with large differences in their respective valence bandwidth, such as alkali metals on Al.[6,7] In these cases, the electronic confinement is induced, without a barrier, by the reflection and transmission of the wave function at the reflection point (Z_R in Fig. 1). The Ag/Al(100) system [Fig. 1(b)] is somewhat different from the previously studied mQW, since it is now the overlayer which displays a bulk energy band gap over the energy range being explored. It is surprising to find electronic resonances in this band gap region in the first place, because no surface states exist for the semi-infinite crystal[11] and second because the discontinuity in the potential responsible for this effect is almost 11 eV below the actual resonance.

The Al(100) crystal was subjected to several cycles of Ar+ sputtering (1 keV) and annealing up to 400 °C, for a total time of approximately 20 h. The crystalline order and cleanliness of the surface were monitored by using both low-energy electron diffraction (LEED) and normal incidence IPS. The Ag layers were deposited from an *e*-beam evaporator with a control feedback loop to obtain a stable deposition rate close to 0.12 ML min^{-1}, 1 ML being the number of atoms necessary to form a uniform (100) layer. The samples were kept close to liquid nitrogen (LN_2) temperatures during deposition, and were subsequently annealed to room temperature. The Ag coverage was verified with a quartz crystal balance. Room-temperature micrographs were obtained with an ultrahigh vacuum (UHV)-scanning tunneling microscope (STM) attached to the UHV system. We have used (IPS), in the isochromat mode,[12] to detect the effects of the interface in the unoccupied electronic states between the Fermi level ε_F and the vacuum level.

Figure 2 shows a set of normal incidence IPS spectra for

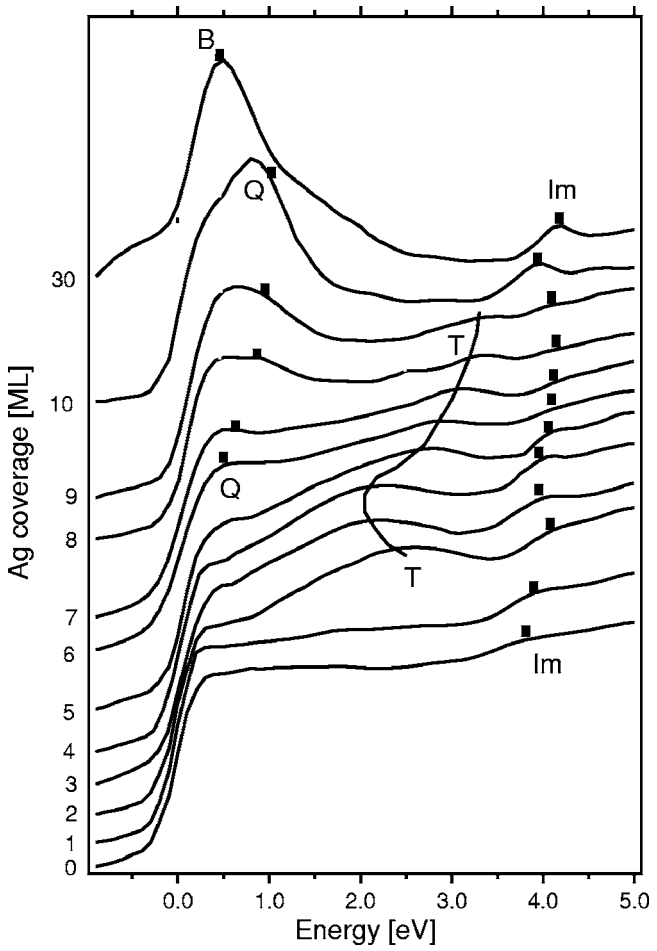

FIG. 2. Set of normal incidence IPS spectra for different Ag coverages. (ε_F) corresponds to 0 eV in the energy axis. The two main resonances have been labeled as Q and T. Q has been identified as a QW-type state and T as resonant tunneling state. B is a bulk-derived feature.

different Ag coverages. The clean Al surface displays a spectral feature close to the vacuum level at 3.8 eV. This feature has been identified[13] as an image state resonance. These types of image states are pinned to the vacuum level, and so their fluctuations as a function of coverage have been linked to changes in work function.[14]

The resonance we have labeled as Q appears at ε_F around 6 ML and disperses up in energy as the Ag coverage increases. It is very strong for 10 ML; beyond this coverage it decreases in intensity, until the dominant feature for 30 ML is the Ag bulk state we have labeled as B. A second resonance, T, appears at coverage of 2 ML, 2.5 eV above ε_F. As the Ag coverage increases, this feature disperses down in energy until 4 ML. From 5 ML up, it decreases in intensity and moves to a higher energy up to a coverage of 9 ML. At 10 ML this feature is no longer detectable. This resonance is peculiar to the Ag overlayer and is not present in Ag(100).[11]

Since the lattice parameters of both Ag and Al differ by only a small amount ($<1\%$), one could in principle expect a layer-by-layer growth of a slightly strained Ag layer at low coverages. The measured LEED diagrams show a (1×1) pattern for coverages up to 3 ML, with a very faint (1×5)

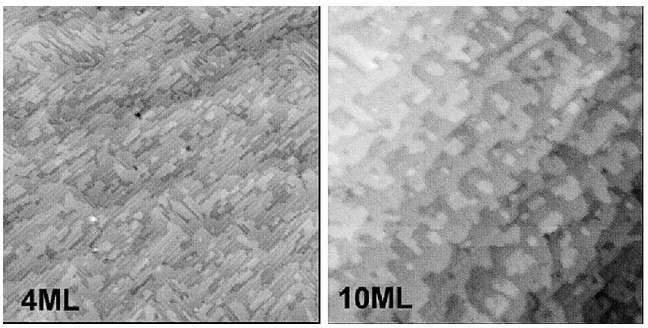

FIG. 3. 200×200 nm^2 STM images for 4- and 10 ML Ag. Layers were deposited close to LN_2 temperature with a rate of 0.12 ML min^{-1}. Both of them show a layer-by-layer structure.

structure[15] at low energies. For coverages between 4 and 7 ML, the LEED intensity shows only a high background at all electron energies. A clear (1×1) pattern re-emerges at coverages higher than 8 ML. STM images of the Ag growth process on Al(100) confirm that the absence of clear LEED maxima is due to an increased disorder rising from dislocations in the overlayer. However, the Ag overlayer growth, under these conditions, i.e., LN_2 temperature and slow deposition rate, remains layer by layer (Fig. 3).

Following the previous work of Barman *et al.*[5] on Na/Al(111), we constructed a simple two-step potential [Fig. 1(b)] in addition to an image barrier potential[17] to describe the valence electronic states in the interface region. In Fig. 4, we show both the Ag and Al density of states (DOS), with a common energy axis, shifted so both metals display the same ε_F. It is then clear that the potential energy presents a 3 eV step at the interface. By solving the 1D Schrödinger's equation numerically using this potential energy, we found indeed several quantum step resonances; however, they did not follow closely the experimental data shown in Fig. 2. One of

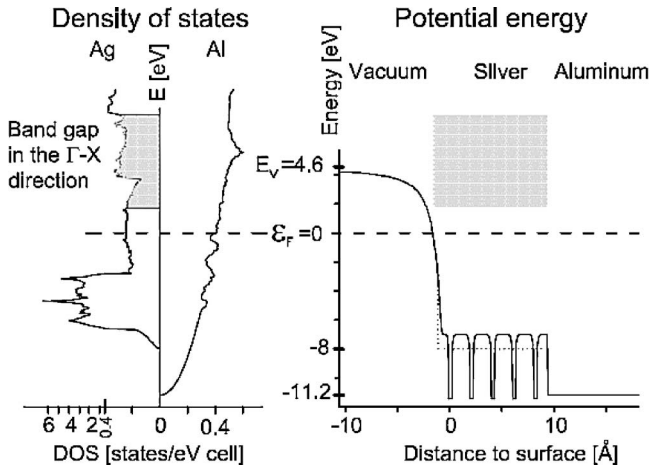

FIG. 4. Right panel: back-to-back representation of the DOS (Ref. 16) of both Al and Ag with a common value for ε_F. The higher intensity around -5 eV in Ag corresponds to the $4d$ electrons. In the left panel we show the two-step potential, with the added Ag atomic corrugation, which we have used to describe the effective interaction of the valence-band electrons with the solid in the overlayer.

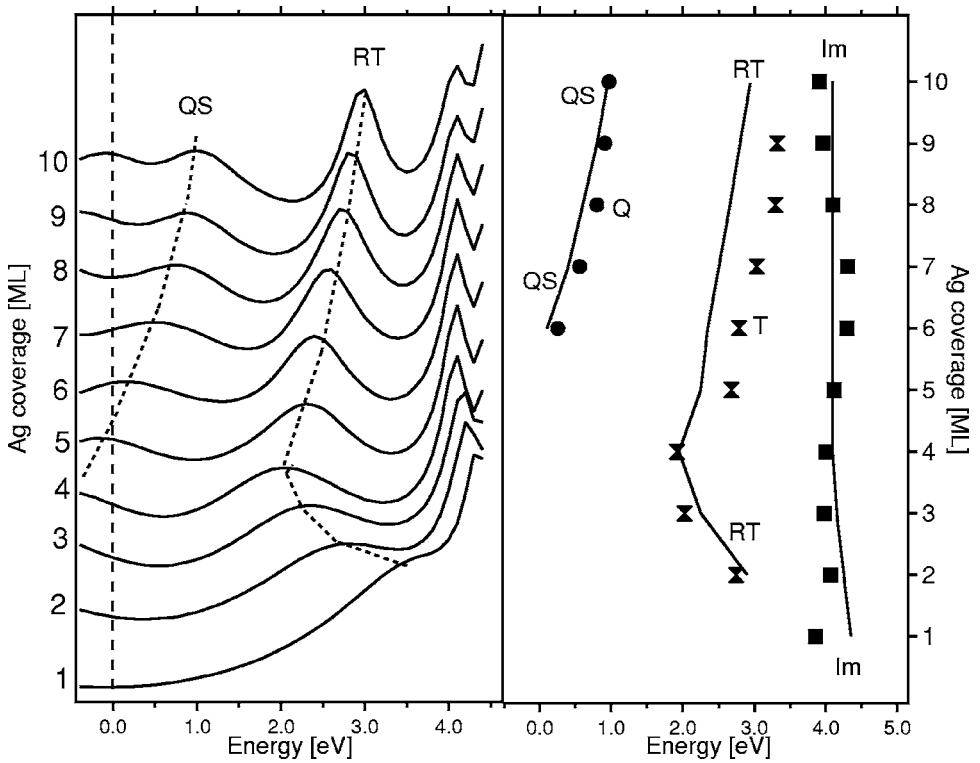

FIG. 5. The left panel shows the calculated spectral quantity R for different coverages. Two dispersing resonances, *QS* and *RT*, can be identified from the calculation. In the right panel we show a comparison between theoretical and experimental energies of the spectral features as a function of the Ag coverage.

the reasons for this disagreement is that the measurements were done in a spectral region including a bulk band energy gap of Ag(100) (from 1.6 to 7.2 eV above ε_F).

A second model we considered included a corrugation in the Ag crystal potential (Fig. 6), to account for the influence of the band gap. For this phenomenological potential, the average value of the corrugated Ag potential energy is now displaced from the Ag *sp* valence-band onset. The corrugation in the potential has the appropriate interatomic distance, and the single ionic potential is modeled by a truncated trigonometric function, parametrized by the width of the core and its depth. The only adjustable parameter in the calculations shown in Fig. 5, changed as a function of Ag coverage, is the position of the image plane[17] relative to the first atomic layer. The rationale behind this image plane shift relates to changes in the surface roughness during early growth. The image plane position has a maximum variation of 1.2 Å, and follows closely the changes of the surface atomic roughness displayed in our STM images.[18]

We have chosen to present the solution to this model as a ratio (R), between the probability of finding the excited electrons in the Ag overlayer, and the probability of finding it in the Al substrate

$$\left[R = \left(\int_{Z_{min}}^{Z_R} |\psi_{Ag}|^2 \right) \Big/ \left(\int_{Z_R}^{Z_{max}} |\psi_{Al}|^2 \right) \right].$$

Since the amplitude of the wave function in the Al region is a constant, this ratio is then proportional to the DOS in the Ag overlayer. It is then susceptible to direct comparison to the measured photon intensities shown in Fig. 2. In the left panel of Fig. 5 we have shown the calculated values of R as a function of energy for each layer thickness. A peak in this spectral ratio can then be interpreted as an overlayer resonance. In the right panel of Fig. 5 we have plotted the energy of the experimental peaks (Q, T, and Im) as a function of coverage, together with the solid lines showing the dispersion of calculated resonances (*QS* and *RT*). From the coincidence between calculation and experiment, it is then natural to associate resonance Q with *QS*. There is also a good agreement with the experiment in the case of the image resonance. When comparing the experimental resonance T with the calculated feature *RT*, the agreement is not as good, since for large coverages the calculation always underestimates the energy of the resonance. Nevertheless, the qualitative dispersion of both features bears close resemblance. In Fig. 6, we show a couple of characteristic solutions for this effective 1D model for 8 ML Ag coverage. The two electronic states shown, one with energy 0.8 eV above ε_F (*QS*) and the other at 3.15 eV (*RT*), correspond to local maxima of the probability of finding an excited electron in the Ag overlayer.

QS has been associated with a pseudo-QWr, since its wave function has zeros at the extreme of the confining potential and it displays an envelope function as shown in QWr; nonetheless, this state has a nonzero amplitude, far into the Al substrate. *RT* has been identified as a resonant tunneling of a surface state. The exponential decay of *RT*, until it reaches the substrate, relates to the fact that this feature appears in the Ag energy band gap, along the surface normal. The QWr character of this state is given by the fact that the

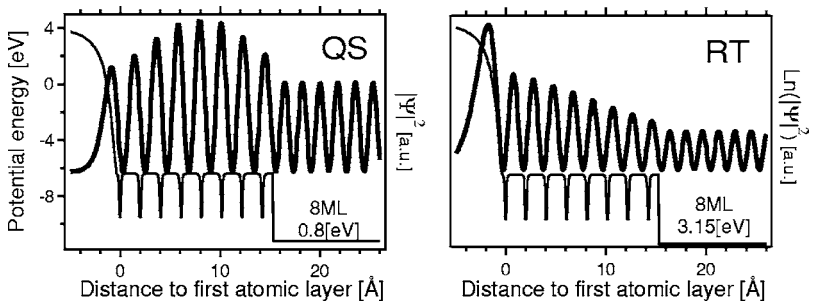

FIG. 6. Square of selected wave functions solution to the 1D model for 8 ML (thick line). The left panel is related to the experimental feature Q, and has the general shape of a QWr. The left panel corresponds to a state with a dispersion similar to the experimental feature T, displaying a resonant tunneling behavior. The thin solid lines correspond to the model of the electronic potential energy.

wave function is also zero at the interface point (Z_R).

At 10 ML (Fig. 3), the STM image shows flat terraces without structures. The LEED diagram at this particular coverage displays again a (1×1) pattern and feature *RT* is absent from the IPS spectra. At lower coverages, the average surface atomic roughness is larger. It has a maximum value between 3 and 4 ML, where *RT* reaches its lowest energy value. Hence, the thickness dependence of the energy of this state seems to correlate well with the atomic roughness of the overlayer.

Since we are using a phenomenological potential, there are many features of the potential itself which could be parametrized to improve the fitting of the data. The important aspect of these results is that the type of solutions we have described (*QS* and *RT*) is very robust with respect to dramatic modifications of the atomic corrugation of the Ag potential within the overlayer. The exact energy for each resonance may change and so would the agreement with the experimental results, but the spatial dependence of the numerical solutions remains the same.

Measurements performed in the off-normal configuration, for several coverages, were done with the purpose of exploring the energy dependence of the spectral features as a function of $k_{\parallel}$. Our results indicate, as expected, a parabolic dispersion with effective electronic masses close to unity for all coverages.[18]

It is clear to us that any further theoretical effort in this system should include a first-principle calculation of the surface–interface electronic structure. In summary, we have measured the dispersion and identified two types of resonances, both linked to barrier-less quantum confinement in the unoccupied electronic spectra of thin Ag atomic layers grown on Al. One of these states displays a resonant tunneling behavior, since it develops within the Ag overlayer energy band gap.

We thank H. Novak and P. Vargas for interesting discussions regarding the 1D-Ag electronic potentials and M. Flores for his help in obtaining the STM images. This research received financial support from FONDECYT (Grant 1030198), Fundación Andes (Grant C-10810/2), and Millennium Sci. Initiative (Grant P02-054-F), Chile.

*Electronic address: patricio.haberle@usm.cl

[1] J. E. Ortega, F. J. Himpsel, G. J. Mankey, and R. F. Willis, Phys. Rev. B **47**, 1540 (1993).

[2] K. L. Man, Z. Q. Qiu, and M. S. Altman, Phys. Rev. Lett. **93**, 236104 (2004).

[3] J. J. Paggel, D.-A. Luh, T. Miller and T.-C. Chiang, Phys. Rev. Lett. **92**, 186803 (2004); H. Sasaki, A. Tanaka, S. Suzuki, and S. Sato, Phys. Rev. B **70**, 115415 (2004); M. Kralj, P. Pervan, M. Milun, T. Valla, P. D. Johnson, and D. P. Woodruff, *ibid.* **68**, 245413 (2003); A. Ernst, J. Henk, M. Lüders, Z. Szotek, and W. M. Temmerman, *ibid.* **66**, 165435 (2002).

[4] I. Matsuda and H. W. Yeom, J. Electron Spectrosc. Relat. Phenom. **126**, 101 (2002); C.-S. Jiang, H.-B. Yu, X.-D. Wang, C.-K. Shih, and Ph. Ebert, Phys. Rev. B **64**, 235410 (2001).

[5] S. Å. Lindgren and L. Walldén, Phys. Rev. Lett. **59**, 3003 (1987).

[6] S. Å. Lindgren and L. Walldén, Phys. Rev. B **38**, 10044 (1988).

[7] S. R. Barman, P. Häberle, K. Horn, J. A. Maytorena, and A. Liebsch, Phys. Rev. Lett. **86**, 5108 (2001).

[8] M. H. Upton, C. M. Wei, M. Y. Chou, T. Miller, and T. C. Chiang, Phys. Rev. Lett. **93**, 026802 (2004).

[9] A. G. Danese, H. Yao H, D. A. Arena, M. Hochstrasser, J. G. Tobin, and R. A. Bartynski, Phys. Status Solidi B **241**, 2358 (2004).

[10] L. Aballe, C. Rogero, P. Kratzer, S. Gokhale, and K. Horn, Phys. Rev. Lett. **87**, 156801 (2001).

[11] N. V. Smith, Phys. Rev. B **32**, 3549 (1985).

[12] P. Häberle, W. Ibañez, R. Esparza, and P. Vargas, Phys. Rev. B **63**, 235412 (2001).

[13] J. F. Veyan, W. Ibañez, R. A. Bartynski, P. Vargas, and P. Häberle, Phys. Rev. B **71**, 155416 (2005).

[14] J. J. Paggel, C. M. Wei, M. Y. Chou, D.-A. Luh, T. Miller, and T.-C. Chiang, Phys. Rev. B **66**, 233403 (2002).

[15] R. J. Smith (private communication).

[16] LMTO calculations of the density of states of Al and Ag provided by P. Vargas.

[17] R. O. Jones, P. J. Jennings, and O. Jepsen, Phys. Rev. B **29**, 6474 (1984); N. V. Smith, C. T. Chen, and M. Weinert, *ibid.* **40**, 7565 (1989).

[18] M. Flores, J. F. Veyan, and P. Häberle (unpublished).